

# Moiré Fringe Phase Difference Measurement Based on Spectrum Zoom Technology

Li Chang\*, Gai Cui

School of Information Science and Engineering, Shenyang University of Technology  
No.111 Shenliao West Road, Economic and Technical Development Zone, Shenyang,  
Liaoning Prov. PR China. 110870

\*Corresponding author, e-mail: changlianli@163.com, sgdjiance2004@163.com

## Abstract

Grating displacement measurement technique is an important means to achieve precise displacement measurement of nanometer scale. Moiré fringe phase difference measurement is the basis of grating displacement measurement technique. Traditional Moiré fringe subdivision method based on DFT algorithm has low frequency resolution relatively when extracting Moiré fringe fundamental frequency spectral line, which causes frequency and phase measurement errors of Moiré fringe fundamental frequency. CZT spectrum zoom technique can improve the frequency resolution of frequency band near Moiré fringe fundamental frequency and get fundamental frequency spectrum lines more exactly, which can solve the problem of low frequency resolution of DFT. The paper studies the relation of Moiré fringe phase difference and grating displacement, and analyzes the working principles of DFT and CZT spectrum zoom method. DFT and CZT spectrum zoom are used for Moiré fringe spectrum analysis and phase difference calculation respectively. Simulation results show measurement error of Moiré fringe phase difference with DFT algorithm is in  $10^{-3}$  degree scale, while measurement error with CZT spectrum zoom algorithm is approximate 0 degree. The comparison results show CZT spectrum zoom method has better performance and applicability, which improves the phase difference measurement accuracy of Moiré fringe effectively.

**Keywords:** Moiré fringe, DFT, CZT spectrum zoom, phase difference measurement.

Copyright © 2013 Universitas Ahmad Dahlan. All rights reserved.

## 1. Introduction

Grating displacement measurement technique is widely applied in the fields of superfinishing and numerical control. With the development of science and technology, displacement measurement technique has entered into nanometer scale measurement times. As the foundation of grating displacement measurement, Moiré fringe subdivision technology can improve displacement measurement resolution and measurement accuracy, which is the most effective way to achieve nanometer scale grating displacement measurement. Moiré fringe subdivision methods include phase subdivision and amplitude subdivision. In 1982, M. Takada published the Moiré fringe subdivision method with Fourier transform [1], which analyzed Moiré fringe signal components in frequency-domain the first time and got higher grating displacement accuracy by improving Moiré fringe phase difference measurement accuracy.

The paper analyzes the grating displacement measurement principle based on Moiré fringe phase difference and the measurement effect of Fourier transform subdivision method, then utilizes CZT (Chirp Z Transform) spectrum zoom technique to calculate the phase difference of Moiré fringe fundamental frequency to ameliorate the measurement result.

## 2. Moiré Fringe Displacement Measurement Principle

Grating displacement sensor consists of light source, main grating, indicative grating and photoelectric conversion elements, in which main grating and indicative grating are superimposed with angle  $\theta$  in space to form the grating pair. The grating pitch is in micron scale and two gratings locate closely, so optic interference phenomenon will occur to generate Moiré fringe when light passes through the grating pair [2, 3].

Moiré fringe has an amplification effect to grating pitch and can reduce the measurement error caused by the non-uniformity of grating pitch, which is important for the realization of precise grating displacement measurement. The distribution of Moiré fringe light intensity is associated with imaging position and imaging time. The law of Moiré fringe light intensity distribution at  $(x, y)$  of time  $t$  is shown as Eq.1 [4, 5].

$$I(x,y,t)=I_1(x,y,t)+I_2(x,y,t)\cos\varphi(x,y,t) \quad (1)$$

Where,  $I(x,y,t)$  is Moiré fringe light intensity distribution.  $I_1(x,y,t)$  is the background light intensity.  $I_2(x,y,t)$  is amplitude of light intensity variation.  $\varphi(x,y,t)$  is Moiré fringe phase.

Grating displacement sensor generates vertical Moiré fringes. Known from the characteristic of vertical fringes, the light intensity is constant in  $y$  direction, and just changes periodically in  $x$  direction, so Eq.1 is equivalent to Eq.2 [6].

$$I(x,t)=I_1(x,t)+I_2(x,t)\cos\varphi(x,t) \quad (2)$$

Sampling Moiré fringe light intensity in  $x$  direction can extract the variation of fringe light intensity. Sample the Moiré fringe light intensity of position  $x$  with high-speed photoelectric conversion element. When the sampling interval  $\Delta t$  is short enough to ensure the phase difference of adjacent sampling fringe less than  $\pi/2$ , the phase difference  $\Delta\varphi_i$  of adjacent sampling fringe can be calculated with Eq.3.

$$\Delta\varphi_i=\varphi(x,t_i)-\varphi(x,t_{i-1}) \quad (3)$$

Where,  $\varphi(x,t_i)$  and  $\varphi(x,t_{i-1})$  are Moiré fringe phase of time  $t_i$  and  $t_{i-1}$ .

When Moiré fringe light intensity is sampled  $N$  times from time  $t_0$  to  $t$ , the Moiré fringe phase variation  $\Delta\varphi$  relative to the initial measurement time  $t_0$  can be figured out with the accumulation of all phase difference  $\Delta\varphi_i$ .

$$\Delta\varphi=\sum_{i=1}^N \Delta\varphi_i \quad (4)$$

Grating movement leads to Moiré fringe phase changing, so the corresponding grating displacement can be calculated with the relation between grating displacement and Moiré fringe phase difference in Eq.5 [7].

$$\Delta x=\frac{\Delta\varphi}{2\pi} \cdot d \quad (5)$$

Where,  $\Delta x$  is grating movement displacement.  $d$  is grating pitch.

The relation of grating displacement and Moiré fringe phase difference is not only in quantity, but also in moving direction. From the analysis above, utilizing interference Moiré fringe and sampling real-time light intensity of Moiré fringe can calculate the Moiré fringe phase difference and grating movement displacement. Therefore, the calculation accuracy of Moiré fringe phase difference is essential to grating displacement measurement.

### 3. Moiré Fringe Phase Difference Measurement Methods

Moiré fringe phase difference measurement includes digital method and analog method, of which digital method usually has more measurement advantages, so utilize digital spectrum analysis technique to calculate the Moiré fringe phase difference. Traditional DFT algorithm and CZT spectrum zoom algorithm are analyzed in Moiré fringe phase difference calculation respectively as follows.

### 3.1. Discrete Fourier Transform Method

DFT algorithm is widely applied in digital signal processing field, which can analyze time-domain signals in frequency-domain and achieve the signal spectrum discretization[8,9]. When the sampling of photoelectric conversion element to Moiré fringe light intensity meets the spatial sampling theorem, the distribution law of Moiré fringe light intensity in Eq.2 is equivalent to Eq.6.

$$I(x,t)=I_0(x,t)+I_1\cos(2\pi f_0x+\varphi(x,t)) \quad (6)$$

Where,  $f_0$  is fundamental frequency of Moiré fringe light intensity variation in  $x$  direction.

Moiré fringe light intensity is periodic signal, and periodic signal can be expanded into Fourier series as Eq.7.

$$f(x)=a_0+\sum_{n=1}^{\infty}(a_n\cos nx+b_n\sin nx)=a_0+\sum_{n=1}^{\infty}A_n\sin(nx+\varphi_n) \quad (7)$$

Where,  $a_0$  is constant term.  $A_n$  is the amplitude of each harmonic wave.  $\varphi_n$  is the initial phase of each harmonic wave.

Eq.7 shows a periodic function consists of constant term and harmonic wave compositions. According to the sampling Moiré fringe data in a Moiré fringe period, the fringe light intensity parameters of  $a_0$ ,  $A_n$  and  $\varphi_n$  can be calculated. For Moiré fringe light intensity signal, the phase of fundamental frequency is associated with grating displacement, so DFT of Moiré fringe light intensity data is processed to extract the fundamental frequency spectral line. The DFT results of Moiré fringe sequence are complex numbers, which are shown as Eq.8.

$$X(k)=\sum_{n=0}^{N-1}x(n)e^{-j(\frac{2\pi}{N})nk}=\text{Re}[X(k)]+j\text{Im}[X(k)] \quad (8)$$

Where,  $x(n)$  is  $N$ -point finite-length sequence of Moiré fringe data.  $\text{Re}[X(k)]$  is the real part of Moiré fringe frequency.  $\text{Im}[X(k)]$  is the imaginary part of Moiré fringe frequency.  $k$  is serial number of spectral lines.

The amplitude spectrum  $A_k$  and phase spectrum  $\varphi_k$  of Moiré fringe light intensity can be obtained with Eq.9.

$$A_k=\sqrt{\text{Re}[X(k)]^2+\text{Im}[X(k)]^2}, \quad \varphi_k=\arctan\frac{\text{Im}[X(k)]}{\text{Re}[X(k)]} \quad (9)$$

Moiré fringe fundamental frequency spectral line has the biggest power spectrum. Extracting the fundamental frequency spectral line can calculate the Moiré fringe fundamental frequency phase of the sampling time. Moiré fringe fundamental frequency phase difference of sampling interval  $\Delta t_i$  can be calculated with Eq.10.

$$\Delta\varphi_i=\varphi_i-\varphi_{i-1}=\arctan\left(\frac{\text{Im}[X_i(k)]}{\text{Re}[X_i(k)]}\right)-\arctan\left(\frac{\text{Im}[X_{i-1}(k)]}{\text{Re}[X_{i-1}(k)]}\right) \quad (10)$$

However, the accuracy of DFT frequency analysis is restrained by inherent barrier effect. DFT frequency resolution is reciprocal with the length of sampling data. If the frequency resolution needs to improve, the sampling time also needs to be increased to get more sampling data, which will lead to a substantial increase of system computation quantity. Therefore, the measurement effect of DFT algorithm in Moiré fringe phase difference measurement is not outstanding. And CZT spectrum zoom technique is applied in Moiré fringe phase difference measurement to improve the defects of DFT algorithm.

### 3.2. Chirp Z Transform Spectrum Zoom Method

Spectrum zoom technique is an important means in signal analysis, which can analyze the frequency structure of a selected frequency region with specified and sufficiently high frequency resolution [10]. Spectrum zoom technique mainly contains Zoom FFT algorithm and CZT algorithm. CZT spectrum zoom algorithm takes dense values in refinement frequency band, increases the amount of frequency analysis points, and calculates the amplitude and phase information of corresponding frequency points.

CZT spectrum zoom algorithm can be used to calculate the z-transform of a fixed path in z-plane. If the fixed path is a circular arc on the unit circle, increasing the output points to make it more than input points, the specified frequency band can be subdivided. For N-points sequence  $x(n)$ , if the sampling data  $z_k$  locate on the unit circle with equal interval of N-points, the z-transform is DFT in this case, so DFT can be regarded as a special case of z-transform. The sampling point  $z_k$  of common path in z-plane can be expressed as Eq.11.

$$z_k = AW^{-k} \quad (11)$$

Where,  $k=0,1,\dots,M-1$ .  $M$  is complex spectrum analysis points.  $A$  and  $W$  are random complex numbers, which can be expressed as Eq.12.

$$A = A_0 e^{j\theta_0}, \quad W = W_0 e^{-j\varphi_0} \quad (12)$$

So the sampling data  $z_k$  can be expressed as Eq.13.

$$z_k = A_0 e^{j\theta_0} W_0^{-k} e^{jk\varphi_0} = A_0 W_0^{-k} e^{j(\theta_0 + k\varphi_0)} \quad (13)$$

Where,  $A_0$  is the vector radius length of initial sampling point  $z_0$ .  $\theta_0$  is the phase angle of initial sampling point  $z_0$ .  $\varphi_0$  is the angle difference of adjacent sampling points.  $W_0$  is the extensional proportion of sampling spiral.  $k=0,1,2,\dots,M-1$ .

Figure 1 shows the corresponding curve of sampling point  $z_k$  in z-plane [11].

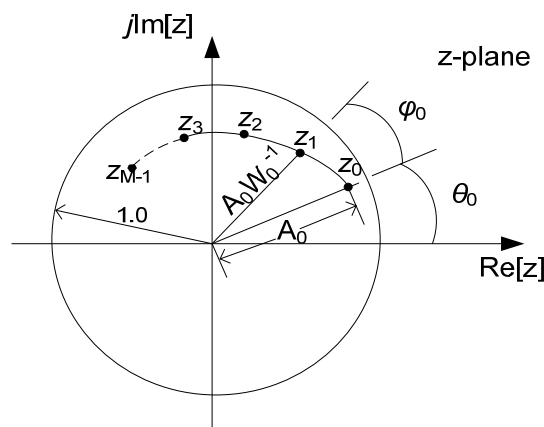


Figure 1. Curve of CZT sampling point  $z_k$  in z-plane

The sampling data  $z_k$  has the following characteristics.

(1) When  $A_0 < 1$ , the sampling spiral locates inside the unit circle, while when  $A_0 > 1$ , the sampling spiral locates outside the unit circle.

(2) When  $W_0 < 1$ , the sampling spiral rotates inside, while when  $W_0 > 1$ , the sampling spiral rotates outside.

(3) When  $A_0 = W_0 = 1$ , the CZT path is a arc of the unit circle, the amount of processing data  $M$  can be different from the input sequence points  $N$ .

CZT of D multiples is dividing the original frequency resolution into D parts equally to get more spectral lines. The closer the spectral lines locate to the spectral peak, the smaller errors frequency calculation result has, and the phase and phase difference calculation results have smaller error too. So CZT spectrum zoom can also be regarded as a correction method, which achieves phase correction by frequency correction.

If the calculation error of DFT algorithm is caused by barrier effect, CZT algorithm can reduce the measurement error and improve the measurement accuracy with the processing of frequency subdivision. But if severe spectral interference phenomenon happens, CZT algorithm can't separate the interfering frequency component and eliminate the effect of measurement error, because CZT spectrum zoom just enlarges a part of frequency band on the frequency axis. In this case, the measurement error can be reduced by adding the original sampling points to improve the original frequency resolution. The z-transform of  $z_k$  is:

$$X(z_k) = \sum_{n=0}^{N-1} x(n)z_k^{-n} = \sum_{n=0}^{N-1} x(n)A^{-n}W^{nk} \tag{14}$$

Known from the Bluestein equality of Eq.15, Eq.16 can be deduced.

$$nk = \frac{1}{2}[n^2 + k^2 - (k-n)^2] \tag{15}$$

$$\begin{aligned} X(z_k) &= \sum_{n=0}^{N-1} x(n)A^{-n}W^{\frac{n^2}{2}}W^{\frac{(k-n)^2}{2}}W^{\frac{k^2}{2}} = W^{\frac{k^2}{2}} \sum_{n=0}^{N-1} [x(n)A^{-n}W^{\frac{n^2}{2}}]W^{\frac{(k-n)^2}{2}} = W^{\frac{k^2}{2}} \sum_{n=0}^{N-1} g(n)h(k-n) \\ &= W^{\frac{k^2}{2}} [g(n)*h(n)] \end{aligned} \tag{16}$$

Where,

$$g(n) = x(n)A^{-n}W^{\frac{n^2}{2}}, \quad h(n) = W^{\frac{n^2}{2}} \tag{17}$$

In Eq.16, z-transform of  $z_k$  can be calculated with linear convolution of  $g(n)$  and  $h(n)$ , then multiplied by  $W^{\frac{k^2}{2}}$ . The z-transform calculation structure is shown in Figure 2.

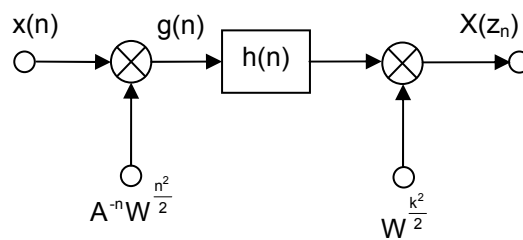


Figure 2. Calculation structure of z-transform

Therefore, for the fixed parameters of  $A_0$ ,  $\theta_0$ ,  $\phi_0$  and  $W_0$ , z-transform of  $z_0, z_1, \dots, z_k$  can be processed in z-plane with Eq.12 and Eq.16.

**4. Simulation Analysis**

Moiré fringe signal sequence  $x(n)$  in Eq.2 can be described as Eq.18.

$$x(n)=A+B\cos\left(\frac{2\pi n f}{f_s}+\varphi\right),n=0,1,\dots,N-1 \quad (18)$$

Where, A is direct component. B is signal variation amplitude. f is Moiré fringe frequency.  $f_s$  is Moiré fringe sampling frequency.  $\varphi$  is Moiré fringe initial phase. N is sampling size [12].

When  $A=1$ ,  $B=3$ ,  $f=100\text{Hz}$ ,  $f_s=1000\text{Hz}$ ,  $N=1000$ ,  $\varphi=0^\circ$ , the Moiré fringe sequence  $x(n)$  is:

$$x(n)=1+3\cos\left(2\pi n \cdot \frac{100}{1000}\right) \quad (19)$$

Figure 3 shows the  $x(n)$  waveform of time-domain when  $n \in [1,50]$ .

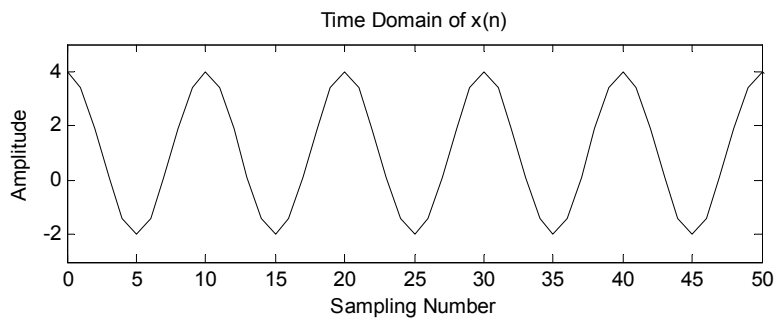


Figure 3.  $x(n)$  waveform of time-domain

Utilize traditional DFT algorithm to analyze the spectrum of Moiré fringe sequence  $x(n)$  in Eq.18. The spectrogram between 95Hz and 105Hz is shown in Figure 4.

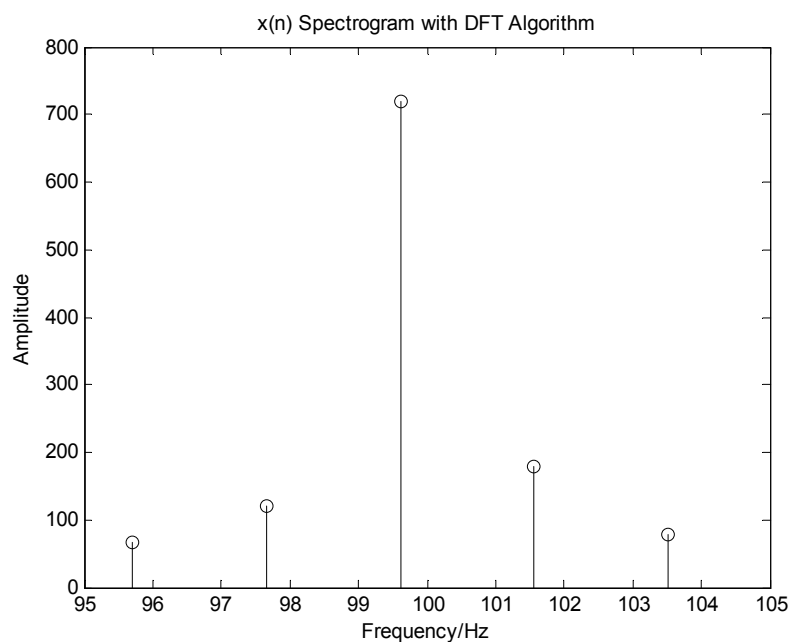


Figure 4. Spectrum analysis of  $x(n)$  with traditional DFT algorithm

In Figure 4, the frequency resolution of  $x(n)$  spectrum analysis with traditional DFT algorithm is 2Hz. The spectral lines figured out don't locate at the frequency point of 100Hz exactly. The spectral line which has the biggest power spectrum is Moiré fringe fundamental frequency spectral line, so the measured Moiré fringe fundamental frequency is 99.6Hz. However, the theoretical Moiré fringe fundamental frequency is 100Hz in Eq.18, traditional DFT algorithm causes 0.4Hz frequency measurement error of Moiré fringe fundamental frequency, which will caused phase difference measurement error of Moiré fringe fundamental frequency further.

Utilize CZT spectrum zoom algorithm to subdivide the frequency band of  $x(n)$  between 95Hz and 105Hz. The processing procedure is described below.

- (1) Determine the subdivision frequency band and the quantity of output data.
- (2) Make the CZT path on the unit circle, determine the positions of the starting point and the ending point, and set the angle difference of adjacent sampling point.
- (3) Calculate the CZT of the sampling points on the path.
- (4) Extract the spectral line of  $x(n)$  fundamental frequency.

The distribution of  $x(n)$  spectral lines between 95Hz and 105Hz is shown in Figure 5.

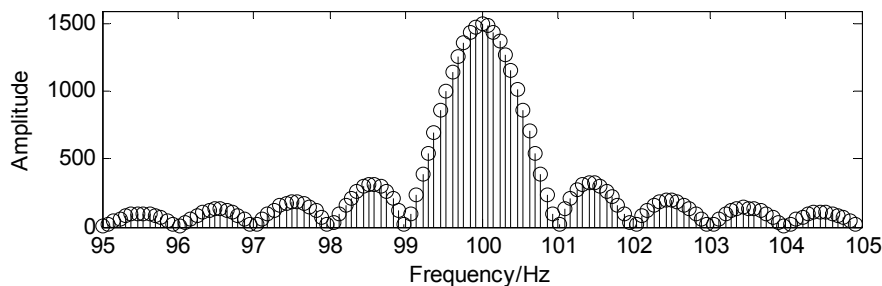


Figure a:  $x(n)$  Spectrum Zoom of CZT with 128 multiples

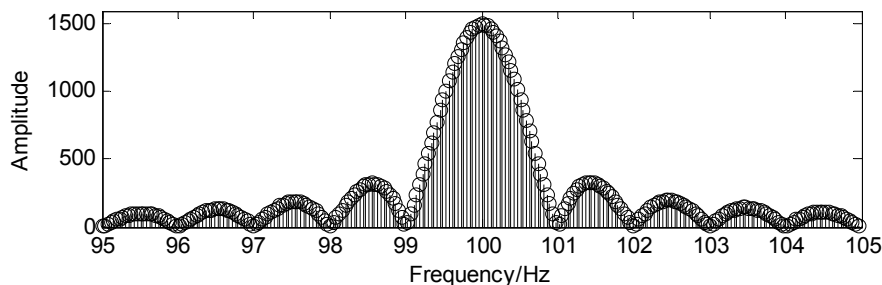


Figure b:  $x(n)$  Spectrum Zoom of CZT with 256 multiples

Figure 5. Spectrum analysis results of  $x(n)$  with CZT spectrum zoom algorithm

In Figure 5, Figure a and Figure b are  $x(n)$  frequency subdivision results of 128 multiples and 256 multiples with CZT spectrum zoom algorithm. The frequency resolution of  $x(n)$  spectrum analysis are 0.078Hz and 0.039Hz respectively, which have more spectral lines between 95Hz and 105Hz than DFT algorithm. The  $x(n)$  spectral line of frequency 100Hz can be extracted exactly. And increasing the subdivision multiples can improve the frequency resolution furthermore. From the contrast of Figure 4 and Figure 5, it can be concluded that CZT spectrum zoom algorithm has prominent spectrum analysis effect for Moiré fringe fundamental frequency spectral line.

When the Moiré fringe initial phase  $\varphi$  of  $x(n)$  in Eq.18 increases  $1^\circ$  each time, utilize DFT algorithm and CZT algorithm respectively to measure the phase difference of each variation of  $\varphi$ . 0-10° is chosen as the Moiré fringe phase variation region, which can obtain 10 groups of phase difference measurement results. The measurement results with two algorithms are shown in Table 1.

Table 1. Moiré Fringe Phase Difference Measurement Results of  $x(n)$  With DFT Algorithm and CZT Algorithm

Group Number	DFT Algorithm (°)	CZT Algorithm (°)
1	0.9966	1.0000
2	0.9968	1.0000
3	0.9968	1.0000
4	0.9970	1.0000
5	0.9970	1.0000
6	0.9972	1.0000
7	0.9972	1.0000
8	0.9974	1.0000
9	0.9975	1.0000
10	0.9976	1.0000

Table 1 shows the Moiré fringe phase difference measurement result of CZT algorithm is more accurate than that of DFT algorithm. Figure 6 shows the measurement error curves of Moiré fringe phase difference measurement with DFT algorithm and CZT algorithm.

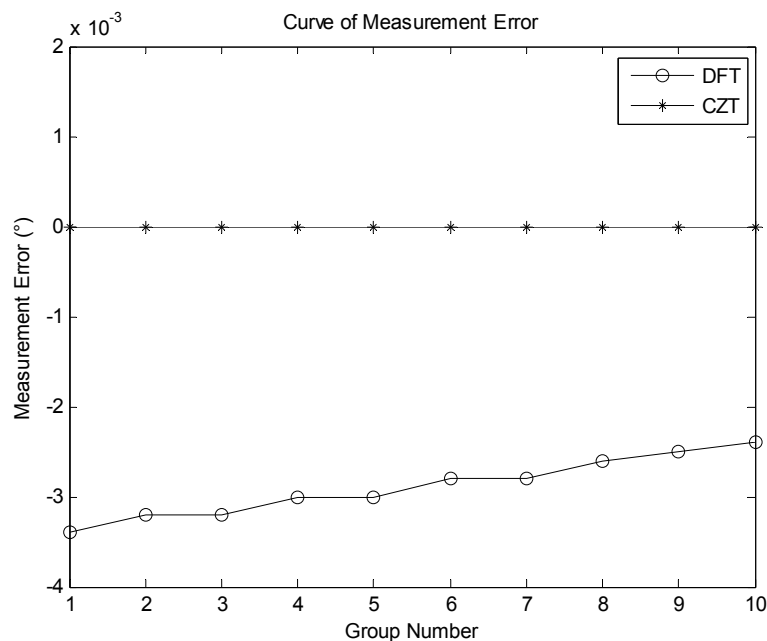


Figure 6. Error curves of Moiré fringe phase difference measurement with DFT algorithm and CZT algorithm

In Figure 6, the average phase difference measurement error of DFT is  $-0.0029$  degree, while the measurement error of CZT spectrum zoom algorithm is approximate 0 degree, which proves the superiority of CZT spectrum zoom technique.

Compared with traditional DFT algorithm applied in Moiré fringe fundamental frequency phase difference calculation, CZT spectrum zoom technique can achieve precise Moiré fringe phase difference measurement without modulation or filtering processing. Besides, the frequency resolution of CZT spectrum analysis is adjusted expediently. Consequently CZT

spectrum zoom technique can reduce Moiré fringe phase difference measurement error, which is benefit for grating displacement measurement.

## 5. Conclusion

Moiré fringe fundamental frequency phase difference measurement effect can affect the accuracy of grating displacement measurement. Traditional DFT algorithm can analyze Moiré fringe fundamental frequency to obtain the phase of Moiré fringe first harmonic wave. However, due to the influence of frequency resolution in spectrum analysis, the phase difference measurement accuracy is relatively low. The application of CZT spectrum zoom technique can solve this problem effectively. CZT spectrum zoom improves the frequency resolution of Moiré fringe spectrum analysis by frequency subdivision, which can obtain exact spectral line of Moiré fringe fundamental frequency for phase and phase difference calculation. Simulation results show the phase difference measurement accuracy of Moiré fringe fundamental frequency with CZT algorithm is higher than that of traditional DFT algorithm. CZT spectrum zoom method can achieve the function of Moiré fringe spectrum correction, reduce frequency and phase measurement errors, and achieve high-precision phase difference measurement of Moiré fringe fundamental frequency, which has a certain significance for precise grating displacement measurement.

## References

- [1] Takeda M, Ma H, Kobayashi S. Fourier-Transform Method of Fringe-pattern Analysis for Computer-Based Topography and Interferometry. *Journal of the Optical Society of America*. 1982; 72(1): 156-160.
- [2] Zhou SL, Fu YQ, Tang XP, Hu S, Chen WF, Yang Y. Fourier-Based Analysis of Moiré Fringe Patterns of Superposed Gratings in Alignment of Nanolithography. *Optics Express*. 2008; 16(11): 7869-7880.
- [3] Periverzov F, Ilies HT. 3D Imaging for Hand Gesture Recognition: Exploring the Software-Hardware Interaction of Current Technologies. *3D Research*. 2012; 3(1): 1-15.
- [4] Ri S, Fujigaki M, Morimoto Y. Sampling Moiré Method for Accurate Small Deformation Distribution Measurement. *Experimental Mechanics*. 2010; 50(4): 501-508.
- [5] Ri S, Muramatsu T, Saka M, Nanbara K, Kobayashi D. Accuracy of the Sampling Moiré Method and Its Application to Deflection Measurements of Large-Scale Structures. *Experimental Mechanics*. 2012; 52(4): 331-340.
- [6] Sciammarella CA, Boccaccio A, Lamberti L, Pappalettere C, Rizzo A, Signore MA, Valerini D. Measurement of Deflection and Residual Stress in Thin Films Utilizing Coherent Light Reflection/Projection Moiré Interferometry. *Experimental Mechanics*. published online, 2013.
- [7] Song N, Ding CH, Liu CH, Quan W. *A Fast Subdividing Research for Grating Signal Based on CPLD*. Communications and Information Processing. Aveiro. 2012; 289: 9-16.
- [8] Zhang Shao-bai, Huang Dan-dan. Electroencephalography Feature Extraction Using High Time-Frequency Resolution Analysis. *TELKOMNIKA Indonesian Journal of Electrical Engineering*. 2012; 10(6): 1415-1421.
- [9] Hui Li, Yingjie Yin. Bearing Fault Diagnosis Based on Laplace Wavelet Transform. *TELKOMNIKA Indonesian Journal of Electrical Engineering*. 2012; 10(8): 2139-2150.
- [10] Reinhold K. Comparison of Frequency Estimation Methods for Reflected Signals in Mobile Platforms. *World Academy of Science, Engineering and Technology*. 2009; 57(1):147-150.
- [11] Fan XH, Zeng XX, Zhang LX, Zhang CQ. Algorithm and Application of Spectrum Zoom Based on Chirp Z Transform. *Journal of Academy of Armored Force Engineering*. 2012; 26(1): 59-62.
- [12] Casavola C, Lamberti L, Pappalettera G, Pappalettere C. *Application of Contouring to Dental Reconstruction*. Conference Proceedings of the Society for Experimental Mechanics Series. New York. 2013; 35: 183-191.